

FORCED CONVECTIVE POST CHF HEAT TRANSFER AND QUENCHING<sup>a</sup>

By:

R. A. Nelson

**DISCLAIMER**

This document contains information that was prepared by an agency of the United States Government for the United States Government but any claim for copyright or other intellectual property rights in the information contained herein shall be the responsibility of the individual or organization that prepared the information. Reference herein to any specific product, process, or service, or to any specific organization, does not imply its endorsement, recommendation, or approval by the United States Government or any agency thereof. The views and opinions of authors expressed herein do not necessarily state or reflect those of the United States Government or any agency thereof.

EG&G Idaho, Inc.  
 P. O. Box 1625  
 Idaho Falls, ID 83415

A paper submitted to the  
 ASME 1980 Winter Annual Meeting  
 Chicago, IL

**MASTER**

a. Work supported by the U.S. Nuclear Regulatory Commission, Office of Nuclear Regulatory Research under Contract No. DE-AC07-76ID01570.

## NOTICE

This report was prepared as an account of work sponsored by an agency of the United States Government. Neither the United States Government nor any agency thereof, or any of their employees, makes any warranty, expressed or implied, or assumes any legal liability or responsibility for any third party's use, or the results of such use, of any information, apparatus, product or process disclosed in this report, or represents that its use by such third party would not infringe privately owned rights. The views expressed in this paper are not necessarily those of the U.S. Nuclear Regulatory Commission.

## ABSTRACT

This paper discusses mechanisms in the post-CHF region which provide understanding and qualitative prediction capability for several current forced convective heat transfer problems. In the area of nuclear reactor safety, the mechanisms are important in the prediction of fuel rod quenches for the reflood phase, blowdown phase, and possibly some operational transients with dryout. Results using the mechanisms to investigate forced convective quenching are presented. Data reduction of quenching experiments is discussed, and the way in which the quenching transient may affect the results of different types of quenching experiments is investigated. This investigation provides an explanation of how minimum wall superheats greater than the homogeneous nucleation temperature result, as well as how these may appear to be either hydrodynamically or thermodynamically controlled. Finally, the results of a parametric study of the effects of the mechanisms upon the LOFT L2-3 hotpin calculation are presented.

## NOMENCLATURE

B	=	constant in film boiling multiplier
C	=	constant in film boiling multiplier
G	=	mass flux
k	=	thermal conductivity
P	=	pressure
q	=	heat flux
t	=	time
T	=	temperature
X	=	quality

### Greek Symbols

$\alpha$	=	void fraction
$\alpha_c$	=	void fraction where $\Delta T_{CHF} = 0$
$\beta$	=	film boiling multiplier
$\Delta T_{sat}$	=	$T_w - T_{sat}$ = wall superheat
$\Delta T_{min}$	=	minimum wall superheat
$\Delta T_{CHF}$	=	wall superheat at CHF

### Subscripts

L	=	liquid
w	=	wall
HN	=	homogeneous nucleation
sat	=	saturation

## 1. INTRODUCTION

This paper qualitatively describes heat transfer mechanisms in the post-CHF region which provide understanding and predictive capability for several current forced convective heat transfer problems. Principle application for this investigation is to quenching phenomena. These mechanisms are particularly important to the nuclear reactor safety area. The mechanisms initiate rod temperature turnaround and quenching during the reflood phase of either a hypothetical loss-of-coolant accident (LOCA) or the FLECHT and Semiscale experiments. The mechanisms are also important to the blowdown phase of a LOCA, as shown by the recent Loss-of-Fluid Test (LOFT) experiments L2-2 and L2-3, (200% cold leg break transients), where core quenching occurred in the early part of the blowdown phase at high (6.9 MPa) pressures. The mechanisms may also be important to certain pressurized water reactor (PWR) operational transients where the reactor may operate in the post-CHF regime for short periods of time. In order to limit maximum cladding temperatures or prevent cladding deformation, accurate prediction of the post-CHF heat transfer including core quench during these transients is of prime importance.

Section 2 provides a brief review of the heat transfer surface technique, associated definitions, and a review of how surface quenching is calculated by current computer codes. The results presented by Grush, et al.<sup>1</sup> on how LOFT L2-3 quenches were predicted are used as an example.

Section 3 discusses the mechanisms in the post-CHF region which produce quenching. These mechanisms are observed in low pressure data and are postulated to also exist at high pressures. The changes in the heat transfer surface resulting from incorporating these mechanisms are discussed.

Finally, results using the new heat transfer surface to investigate forced convective quenching are presented in Section 4. Data reduction of quenching experiments is discussed and the effects the quenching transient

may have on the results of different types of quenching experiments is investigated. Also, a parametric study of the effects of the new heat transfer surface upon the LOFT L2-3 calculations is presented.

## 2. THE HEAT TRANSFER SURFACE TECHNIQUE

The heat transfer surface technique was originally developed for RELAP4/MOD6<sup>2</sup> and was initially presented at an NRC sponsored Heat Transfer Workshop<sup>3</sup>. Results utilizing this concept have been presented by Nelson and Sullivan<sup>4,5</sup> and Bjorden and Griffith<sup>6,7</sup>. The technique was originally a three dimensional plot of heat flux which provided a simple visual means of studying parameter trends of individual heat transfer correlations, or groups of correlations spliced together. This visualization has proven extremely useful in terms of both problem understanding and solution.

This section will discuss the heat transfer surface concept, definitions pertinent to quenching, and utilize the heat transfer surface technique with the LOFT L2-3 results as presented by Grush, et al.<sup>1</sup>, to understand how codes currently predict quenching.

### 2.1 Heat Transfer Surface Concept

The function  $z = f(x, y)$  may be viewed as a surface when  $z$  is plotted as a function of  $x$  and  $y$ . The insight gained from this visual approach can be quite helpful, particularly when a number of functions  $z_1, z_2, \dots, z_N$  must be combined to cover a wide range for the independent variables  $x$  and  $y$ .

This mathematical concept of a surface has been termed "the heat transfer surface" when the functions  $z_1, z_2, \dots, z_N$  are heat transfer correlations and the correlations are considered as functions of  $n$

variables. Thus, the heat flux defined by a number of different correlations is viewed as a function of wall superheat, quality, pressure, mass flux, etc., i.e.,

$$q = q (\Delta T_{\text{sat}}, X, P, G, \dots). \quad (1)$$

To plot the heat flux as a three-dimensional surface, the wall superheat and quality are usually picked as the primary independent variables, with the remaining variables assumed constant, as shown in Figure 1. This choice may be changed to study the sensitivity of the surface to other variables. However, when the wall superheat and quality are used as primary variables, the definition of a "boiling curve", as it is used in this discussion, arises. A boiling curve shows then the dependence of heat flux upon wall superheat with all other variables held constant, as shown in Figure 2.

The heat transfer surface shown in Figure 1 is composed of two families of curves. In addition to the family of boiling curves, there is the family of constant wall superheat curves, which view heat flux as a function of quality and which we will term "isothermal curves." Both families assume all other parameters (independent variables) to be held constant.

To aid the visualization, Figure 3 denotes different areas on the heat transfer surface in terms of classical boiling regimes such as single phase liquid heat transfer, nucleate boiling, transition boiling, film boiling and single phase vapor heat transfer. The slope of the heat transfer surface with respect to wall temperature,  $T_w$ , is positive in all the boiling regimes except for the transition boiling region.

In order to relate the heat transfer surface approach to the "classical boiling curve" as originally proposed by Nukiyama<sup>8</sup>, assume for the moment that Figure 3 can represent a pool boiling situation. The pool

boiling curve can now be shown on the heat transfer surface. For this classical pool boiling curve, the "quality" used is the "average quality at a point on the wall" and is changing as the wall temperature changes. In reality, for the pool boiling situation, there is only a narrow range of qualities, if not just one, for any given wall temperature, so that a full heat transfer surface as originally assumed does not exist. Thus, a unique (or nearly unique) classical pool boiling curve exists for a given material, pressure, wall finish or condition, and geometry. For forced convective heat transfer, a unique classical boiling curve does not exist as it does for pool boiling. Instead, the heat transfer surface may be transversed in an infinite number of ways as determined by the coupled response of the wall and the hydraulics. This non-unique nature of forced convective classical boiling curves will be fully discussed in Section 4.1.

## 2.2 Definitions of Cool Down, Rewetting, Return to Nucleate Boiling (RNB) and Quenching

It is now important to define terms which are used herein during the discussion of quenching. These definitions are presented with respect to a typical boiling curve, as shown in Figure 2. A cooldown of the wall occurs when the wall temperature decreases. This cooldown can take place at any point on the boiling curve as long as the energy being convected out of the wall is greater than the energy being conducted through the material to the wall's surface.

The rewet of a point on the wall is defined as having occurred when a point covered by vapor is once again contacted by liquid. Thus, the rewet of the wall implies a triple interface of solid, liquid and vapor existing at different points on the wall. This definition relates then to a microscopic view of the heat transfer and contains no statement as to the wall temperature at which rewetting occurs. Thus, as observed by Bradfield<sup>9</sup>, rewetting may occur in the film boiling region for wall superheats greater than  $\Delta T_{\min}$ .



Finally, a return to nucleate boiling (RNB) occurs when cool down is sufficient to reach the nucleate boiling region (indicated in Figure 2). This return may be initiated from either the transition boiling region or the film boiling region, depending upon the wall temperature. If the RNB occurs from the film boiling region, the process is defined as a quench.

### 2.3 Current Predictions of Quenching

Current predictions of quenching can be divided into two major cases. The first case is those experiments where quenching is controlled by conduction as a result of poor precursory cooling downstream of the quenching front. The other case is those experiments where precursory cooling is sufficient to cause cooling downstream of the conduction propagating quenching front. While work remains to be done on the first case, it has been extensively studied and an excellent review of this work is provided by Elias and Yadigaroglu<sup>10</sup>. The second case will be concentrated upon here.

For the second case, where precursory cooling downstream of the quenching front is significant, two axial locations are considered. The first location is a point immediately downstream of the conduction propagating quenching front. With sufficient precursory cooling at this point, the speed of the quenching front will be increased<sup>11</sup> and the quenching front might now be termed a "conduction-convective propagating quenching front." The second location will be far downstream of the conduction-convection quenching front. If precursory cooling is sufficient, a "spontaneous" convective quench may occur at this point prior to the arrival of the conduction-convection quenching front. For the moment axial conduction at this point will be neglected, concentrating instead upon the point as quenching begins in order to understand how forced convective heat transfer influences this quench.

In order to investigate how forced convective heat transfer influences the calculated quenches, the results from the Loss-of-Fluid Test (LOFT) L2-3 experiment are used as an example. As discussed by Grush et al.<sup>1</sup>,

quenching in the L2-3 experiment is produced by a two phase, low quality fluid front (density wave) propagating through the core. How the codes currently predict the quench is best understood by first denoting the relative maxima and minima of the heat transfer surface shown in Figure 1. The loci of these points are projected down onto the quality-wall superheat plane and denoted as  $\Delta T_{CHF}$  and  $\Delta T_{min}$  as shown in Figure 4. Quenching is currently produced by the density wave (quality decrease) reestablishing transition boiling ( $\partial q/\partial T_w < 0$ ). This change is shown by a typical quenching path of L2-3 (point A to D) on Figure 4. In order to successfully predict the L2-3 quench, the codes have had to move the  $\Delta T_{min}$  loci out (increase  $\Delta T_{min}$ ) so that the quality decrease produced by the density wave crosses the  $\Delta T_{min}$  line.

### 3. CONVECTIVE POST-CHF HEAT TRANSFER AND QUENCHING

Section 2.3 has discussed how the current post-CHF heat transfer codes predict quenching of the LOFT L2-3 cladding temperatures. This technique of calculating quenches is not unique to the L2-3 results. Similar procedures have been used in reflood calculations<sup>2,12</sup>. It is the purpose of this section to study the post-CHF region and determine how convective quenching is really produced.

#### 3.1 Low Flow - Low Void Film Boiling

The initial step in determining how convective quenches are produced is to realize that the heat transfer mechanisms that occur during the low flow low void post-CHF region, where quenching generally occurs, are not well understood. Recalling the isothermal family of curves which constitute the heat transfer surface, as shown in Figure 1, a typical isothermal line in the film boiling region ( $\partial q/\partial T_w > 0$ ) for current film boiling correlations is shown as the solid line in Figure 5. The heat flux decreases as the quality decreases. The dashed line in Figure 5 represents a synthesized low quality effect on the film boiling regime based on the

low pressure work of Iloeje<sup>13</sup>, Dougall-Rohsenow<sup>14</sup> and Cheng et al.<sup>15</sup>. The current correlations do not have this synthesized characteristic because the data used for their development in the low flow regime is high quality data.

Consider the three papers and the quality regions they cover. Iloeje's three step model for dispersed flow shows an  $X_{min}$ , as noted in Figure 5, to exist in the low flow regime. The increase in heat flux for decreasing quality is produced by those drops which enter the thermal boundary layer (TBL) but do not contact the wall. This increase in heat flux becomes more pronounced as more drops are available to enter the TBL. As quality continues to decrease, Dougall-Rohsenow observed a continuing increase in the heat flux. This increase was attributed to the heat transfer in the inverted annular flow regime. Cheng et al. studied the effects of subcooling on the boiling curves and found an increase in heat flux as the subcooling was increased.

Recent data taken by Barnard et al.<sup>16</sup> and Fung et al.<sup>17</sup> support the synthesized low quality effect in the low flow film boiling region at low pressure, as shown in Figure 6. Barnard et al.<sup>16</sup> also studied the effects of flow rates and found a significant effect for the pressures studied as shown in Figure 7. Both studies show these effects to be in the film boiling region since the  $\partial q / \partial T_w > 0$  and are not the result of entering the transition boiling region ( $\partial q / \partial T_w < 0$ ) due to a quality change as typically shown in Figure 4. It is this low quality effect in the low flow film boiling region which initiates low pressure convection quenches. An example of this type of quenching is seen at the top of the core in the FLECHT forced feed experiments.<sup>18</sup> Once the top of the rod experiences the convective quench, the upper quench front propagates down by conduction-convection to meet the conduction-convection front propagating up from the bottom.

While no data are currently known to be available at higher pressures to validate the low quality, low flow effect, it is believed to be present as pressure increases based on the following argument. While the data and

interpretation to this point have been presented in terms of quality, the void fraction is a better variable for presentation, since it indicates the volume of liquid available to influence the phenomena. As pressure increases, the quality at which the same relative volume of liquid is present increases and the same mechanisms should exist. Just as in the low pressure convective quenches, the same basic effect should initiate high pressure convective quenches. An example of the influence of this type of convective initiated quenching is the LOFT L2-3 blowdown experiment. This example will be discussed in detail in Section 4.1, but it should be noted here that other factors such as external thermocouples and fuel rod modeling may also influence the results.

### 3.2 Wall Temperature for the Onset of Stable Film Boiling

The preceding section has discussed new film boiling characteristics which initiate convective high temperature quenches. While liquid may contact the wall in the film boiling region from a microscopic viewpoint as previously noted, the question arises as to when this contact becomes significant from the macroscopic viewpoint and affects the heat transfer. This section will address that question. As will be discussed in detail in Section 4.1, the methods used in the reduction of much of the current forced convection data makes the direct answering of this question difficult.

Much work has been done in determining how and when significant liquid contact begins. For reviews of the general work in this area, those by Comeau<sup>19</sup> and Fung<sup>20</sup> are useful. To more clearly define our question, recent publications by Gunnerson and Cronenburg<sup>21</sup> and Yao and Henry<sup>22</sup> prove quite useful. Gunnerson and Cronenburg present a generic approach to specifying the onset of stable film boiling, and indicate the temperature is bounded by

$$T_{\text{sat}} < T_i \leq T_{\text{max},s} \quad (2)$$

where

$$T_i = \frac{T_w (k/\sqrt{\alpha})_w + T_L (k/\sqrt{\alpha})_L}{(k/\sqrt{\alpha})_w + (k/\sqrt{\alpha})_L} \quad (3)$$

is the interfacial temperature as defined by Carslaw and Jaeger<sup>23</sup> and  $T_{\max,s}$  is the liquid maximum metastable superheat. Yao and Henry<sup>22</sup>'s work emphasizes the effects of pressure and materials upon two fluids, one of which is water. Their results indicate that for pool boiling on a horizontal surface the minimum film boiling point is determined by the mechanism which is stable to the lowest wall temperature of either the Taylor instability mechanism, or the spontaneous nucleation mechanism. For water, the hydrodynamic instability can be assumed to control at pressures less than 1.5 MPa, and the homogeneous nucleation temperature limit is used at higher pressures<sup>22</sup>. For our case of vertical boiling, the Helmholtz instability should replace the Taylor instability; however, due to the uncertainties in the effects of flows upon this limit, the homogeneous nucleation temperature limit will be assumed to apply for all pressures for simplicity. Thus, the wall temperature at which stable film boiling begins will be assumed to be when the interfacial temperature equals the homogeneous nucleation temperature and is given by

$$T_{w,HN} = \frac{T_{HN} \left[ (k/\sqrt{\alpha})_w + (k/\sqrt{\alpha})_L \right] - T_L (k/\sqrt{\alpha})_L}{(k/\sqrt{\alpha})_w} \quad (4)$$

where  $T_{HN}$  is the homogeneous nucleation temperature of the liquid. With respect to the wall superheat, this wall temperature for the onset of film boiling will be denoted as  $\Delta T_{HN} = T_{w,HN} - T_{sat}$ . Low pressure forced convective results presented by Cheng et. al.<sup>15</sup> support this assumption as a first approximation.

### 3.3 Effects on the Heat Transfer Surface

The effects on the heat transfer surface due to changes in the film boiling region will now be considered. This can be most easily done in terms of the relative maxima and minima for the new heat transfer surface, as shown in Figure 8. Figure 8 replaces the original single minimum of Figure 4,  $\Delta T_{min}$ , with two relative minima,  $X_{min}$  and  $\Delta T_{HN}$ . The  $X_{min}$  loci are those minimum heat flux points determined from results presented typically in Figure 5 when the wall temperature is varied. It denotes when  $\partial q/\partial X$  changes sign. this line is controlled primarily by the hydraulic conditions adjacent to the wall. The  $\Delta T_{HN}$  loci represents the wall temperature below which liquid may contact the wall generally (macroscopically) and separates transition boiling ( $\partial q/\partial T_w < 0$ ) and film boiling ( $\partial q/\partial T_w > 0$ ). This line is controlled primarily by wall material properties, wall finish, and thermodynamic effects. While Figures 4 and 8 have been presented as conceptual plots without definitive numbers, the significant reduction in the area representing the transition boiling region in Figure 8 when compared to Figure 4 is done so to indicate that reduction. The effects of this reduction will be discussed in detail in Section 4.

## 4. THE EFFECTS OF CONVECTIVELY INFLUENCED QUENCHES UPON EXPERIMENTS

This section will be divided into two parts and will address the question of how the phenomena discussed in Section 3 will influence forced convective quenching experiments. The first part will discuss post-CHF data reduction from quenching experiments. The second will discuss the LOFT L2-3 example in terms of the quenches occurring during the blowdown. As noted in Section 2.3, this discussion will limit itself to that class of experiments where precursory cooling downstream of the conduction-convection propagating quench front causes cooldown. It will investigate a point far downstream of the quenching front and will initially neglect axial conduction effects. This last restriction of neglecting axial conduction will later be removed from the discussion.

## 4.1 Post-CHF Data Reduction

The current literature on  $\Delta T_{\min}$  and transition boiling for forced convection provides at best a very confusing picture. Three effects are believed to be the primary contributing factors in this confusion. The first effect is that the data reduction procedure may produce results dependent upon the quenching transient. The second is that different types of experiments have been used. And the third, which has undergone much discussion in the literature, is the effect of axial conduction upon  $\Delta T_{\min}$ .

It is the objective of this section to discuss how the data reduction procedure, quenching transient and axial conduction influenced the results obtained from two general types of experiments. The first type of experiment considered will be forced convective quenching experiments with long tubes and/or bundles. The second will be forced convective quenching experiments using short test sections with high thermal inertia.

4.1.1 Tubes and Bundle Quenching Experiments. Two types of data reduction procedures will be considered. The first is that procedure implied by the "classical boiling curve" approach where heat flux is considered a function of wall superheat neglecting the effects of other changing variables. The second is that procedure defined by the heat transfer surface approach where the boiling curve represents the heat flux as a function of wall superheat with all other variables held constant. In order to investigate data reduction procedures for tubes and bundles, heat flux is written in functional form as denoted in Equation (1).

The "classical boiling curve" approach to data reduction assumes (improperly) that heat flux is only a function of wall superheat. The slope of the boiling curve is given by  $dq/d\Delta T_{\text{sat}}$ . Using Equation (1) and the chain rule, the total derivative of heat flux with respect to wall superheat is given by

$$\frac{dq}{d(\Delta T_{sat})} = \frac{\partial q}{\partial(\Delta T_{sat})} + \left[ \frac{\partial q}{\partial X} \frac{dX}{dt} + \frac{\partial q}{\partial G} \frac{dG}{dt} + \frac{\partial q}{\partial P} \frac{dP}{dt} \right] / \frac{d(\Delta T_{sat})}{dt} \quad (5)$$

where  $t$  is time. Equation (5) indicates how different factors will effect the "classical boiling curve." Thus the "classical boiling curve" for quenching experiments with tubes and bundles is a complex relationship of the heat transfer surface ( $\partial q/\partial \Delta T_{sat}$ ,  $\partial q/\partial X$ , . . .), the hydraulic transient ( $dX/dt$ ,  $dP/dt$ , . . .) and the conduction-convection transient of the wall ( $dT_w/dt$ ).

A special case of the general quenching experiments on tubes and bundles exists in those experiments which are run at constant pressure and inlet mass flux. For this case,

$$\frac{dP}{dt} = \frac{dG}{dt} = 0 \quad (6)$$

so that Equation (5) reduces to

$$\frac{dq}{d\Delta T_{sat}} = \frac{\partial q}{\partial \Delta T_{sat}} + \frac{\partial q}{\partial X} \frac{dX}{dt} / \frac{d\Delta T_{sat}}{dt} . \quad (7)$$

This data reduction procedure yields a minimum wall superheat found from  $dq/d\Delta T_{sat} \equiv 0$  and a transition boiling region where  $dq/d\Delta T_{sat} < 0$ . From Equation (7), it is observed that both the  $\Delta T_{min}$  and transition boiling are both dependent on the experimental transient. Transition boiling will thus appear to occur when for example

$$\frac{dX}{dt} < - \left[ \frac{\frac{\partial q}{\partial(\Delta T_{sat})}}{\frac{\partial q}{\partial X}} \right] \frac{d(\Delta T_{sat})}{dt} . \quad (8)$$



Equation (8) can now be interpreted in terms of the new low flow low void film boiling effect for a typical quenching path as shown in Figure 8. Quality is decreasing as the conduction-convection quench front progresses toward the point being considered. After  $X_{min}$  is crossed, the following relationships exist

$$\frac{\partial q}{\partial (\Delta T_{sat})} > 0, \frac{\partial q}{\partial X} < 0, \frac{d(\Delta T_{sat})}{dt} < 0. \quad (9)$$

so that transition boiling appears to occur when  $dX/dt$  is decreasing at a sufficient rate. Figure 9 is the resulting classical boil curve. Points A through E from Figure 8 are also noted in their appropriate place on Figure 9. Of particular importance are points B and C. Point B denotes when  $X_{min}$  is crossed and Point C denotes when the interfacial temperature drops to the homogeneous nucleation temperature. The apparent  $\Delta T_{min}$  resulting from this interpretation is greater than  $\Delta T_{HN}$  and as shown depends upon the experimental transient.

Another interesting result from this analysis is that the  $\Delta T_{min}$  obtained from an experiment where Equation (8) is satisfied will appear to be hydraulically controlled. However, when the transient does not satisfy Equation (8), i.e., does not decrease the quality fast enough, the resulting  $\Delta T_{min}$  will be  $\Delta T_{HN}$  and the minimum will appear thermodynamically controlled. Similar results are obtained for the more general quenching experiment, only the relationships are more complex.

The heat transfer surface approach to determining boiling curves for the data reduction of quenching experiments using tubes and bundles yields only the heat transfer surface characteristic with respect to wall superheat, i.e.,  $\partial q / \partial \Delta T_{sat} \Big|_{X, G, P = \text{constant}}$ . This must be obtained from the experiment by a transient analysis of the hydraulic conditions as a function of axial position,  $z$ , so that  $X = X(z, t)$ ,  $G = G(z, t)$ , and  $P = P(z, t)$ . Only in this manner can the values of heat flux and wall temperature be selected for constant values of  $X$ ,  $G$  and  $P$ . This analysis

may require the use of a number of experimental runs in order to properly span the desired wall temperature range. If other characteristics of the heat transfer surface are desired a similar procedure must be used. For example the isothermal curves are obtained from  $\partial q / \partial X \Big|_{T_w, G, P = \text{constant}}$ .

With this understanding of how the data reduction procedures influence the convective heat flux results obtained from the quenching of tubes or bundles, the effect of axial conduction can be integrated into our thinking. This integration yields then a picture which applies to either of the two axial locations defined in Section 2.3. Usually, the point located immediately downstream of the quenching front is the location which provides the majority of the data with respect to transition boiling when quenching of a tube or bundle is studied. Unfortunately, this is also the point where axial conduction and the rate of change of the hydraulic transient are the maximum making the analysis of this type experiment very difficult.

4.1.2 Short Test Sections of High Thermal Inertia. The short test section with high thermal inertia with proper prevention of axial conduction provides the advantage that it quenches due to its shortness with "constant" hydraulic conditions defined by the inlet. Thus,

$$\frac{dP}{dt} = \frac{dG}{dt} = \frac{dX}{dt} = 0, \quad (10)$$

so that Equation (5) yields

$$\frac{dq}{d(\Delta T_{\text{sat}})} = \frac{\partial q}{\partial (\Delta T_{\text{sat}})}, \quad (11)$$

for the experiment. The high thermal inertia prolongs the quenching period such that sufficient data can be acquired during the true transition boiling period,  $(\partial q / \partial T_w < 0)$ .

Equation (11) indicates that the results obtained from this experiment will be the same for either of the data reduction procedures discussed in Section 4.1.1. This is an advantage since the results from this type experiment do provide boiling curves immediately useful to the heat transfer surface approach. The problem, if it can be termed that, created by this type experiment has been that its results sometimes disagreed with tube results and confusion has arisen.

#### 4.2 LOFT L2-3 Quenches

Grush et al.<sup>1</sup> have shown that the quench occurring in the first 10 s of LOFT LOCE L2-3 was due to liquid propagating through the core. This quenching phenomena is quite similar to that just discussed in Section 4.1.1. The conceptual initiation of the LOFT quenches can again be represented as shown in Figure 8 by the typical quenching path. As already noted, however, high pressure data where the LOFT quenches occurred are not currently available in order to properly modify the heat transfer surface for low flow low void film boiling. This section presents the results of a parametric study of film boiling changes upon the heat transfer surface and how they affect the calculated fuel rod quench of L2-3 using RELAP4/MOD6. This study allows us to make some observations concerning the LOFT quenches.

Three modifications were made to the RELAP4/MOD6 heat transfer surface. The Biasi CHF correlation<sup>24</sup> was used in order to preserve dryout times consistent with Grush, et al.<sup>1</sup> Transition boiling was modified so that film boiling occurred when the interfacial temperature exceeded the homogeneous nucleation temperature. Finally, a void fraction multiplier was placed upon the Condie-Bengston film boiling correlation<sup>2</sup> originally used in the calculations. This multiplier is given by

$$\beta = \left[ \frac{B}{\alpha_c} (\alpha_c - \alpha)^C + 1 \right] \quad (12)$$

where B and C are constants and  $\alpha_c$  is the void fraction where  $\Delta T_{CHF} = 0$  as shown in Figure 8. This film boiling multiplier does not contain a mass flux effect as Bernard, et al.'s<sup>16</sup> data suggests, since the mass flux during this quenching period is approximately constant at  $100 \text{ kg/m}^2 \cdot \text{s}$ . The void fraction used in this calculation is the homogeneous void fraction (no slip).

Figure 10 presents the results of the parametric study. Since the current correlations should be valid for the high quality region the value of the constant C was selected with this in mind. A value of  $C = 1.2$  is representative of the results obtained and was used in obtaining the results shown in Figure 10.

Figure 10 shows the results of three calculations for the hot pin's hot spot temperature compared to data. The runs used values of  $B = 0, 9, 99$ . At a quality of 20%, which was the lowest value calculated as the liquid propagated through the core, multipliers ( $\beta$ ) of 1.00, 2.01 and 12.16, respectively were computed. With no multiplier ( $B = 0$ ), no quench is predicted. With  $B = 9$ , a cooldown resulted, but no quench occurred. With  $B = 99$ , quench resulted.

Based upon the limited low pressure data available,  $B = 99$ , or a multiplier of about 12 at 20% quality, is believed to be an upper bound upon the increase in heat flux which might result from the low flow, low void effect on film boiling. This result implies that additional effects are probably at work in the LOFT results. These effects include the LOFT external thermocouples (TCs) and fuel rod modeling.

Four external TCs are used in LOFT on each fuel rod selected for measurements. They are placed at  $90^\circ$  intervals around the circumference of the fuel rod and extend the length of the rods. For TCs located high on the rod, dummies extend down the rod to its bottom. The sheath is laser welded to the fuel rod about every 2.5 cm. The scenario for the TC effect is as follows: As the density wave propagates through the core, the low flow, low void effect initiates cooldown of the fuel clad and the TC. Since heat is conducted into the TC primarily through the weld joint,

points on the TC between the welds cooldown faster. These points then quench and cause other points along the TC to quench. This TC quenching propagates back into the fuel rod clad. This "fin" effect of the TC therefore speeds the quenching.

Lin<sup>25</sup> has presented results which show an effect due to fuel rod modeling changes on the fuel rod temperature calculation. These effects arose when the results of RELAP4/MOD6 were compared to FRAP-T5<sup>26</sup> where the heat fluxes from RELAP were used as the thermal boundary condition for FRAP. Additional work needs to be done in order to fully understand the modeling difference between RELAP and FRAP and how they effect the calculation.

## 5. CONCLUSIONS

This paper has presented a study of the quenching of forced convective water systems, which applies to both blowdown and reflood experiments associated with nuclear reactors. A low flow, low void film boiling effect has been found in low pressure data which is believed to extend to high pressures. The point where film boiling begins is defined as the wall temperature at which the interfacial temperature equals the homogeneous nucleation temperature.

Integration of these effects into the heat transfer surface provided a means of further studying how the new post-CHF heat transfer model affected data reduction of different quenching experiments. For the quenching of tubes or bundles both axial conduction and low flow, low void film boiling convective heat transfer confuse the quenching issue. It was shown that without proper separation of the variables apparent values of  $\Delta T_{\min}$  result which are dependent upon the particular quenching transient used in the experiment. Thus, values of  $\Delta T_{\min}$  greater than  $\Delta T_{HN}$  result. Also, both hydraulically controlled and thermodynamically controlled  $\Delta T_{\min}$  values result, depending upon the transient. From these results it is concluded that extreme care must be exercised in the reduction of data from

quenching tubes and/or bundles. For the quenching of short test sections of high thermal inertia, the data reduction was found to be far more straightforward from a convective viewpoint. Care must be exercised, however, in terms of either preventing experimentally or analyzing properly the effects of axial conduction.

Application of the new heat transfer surface to the LOFT L2-3 experiment through a parametric study revealed that, while the low flow, low void film boiling effect initiates the cooldown, it does not appear that it can produce the quench rate shown by the data. This rapid quench is currently believed to be a combination of the external thermocouples used in LOFT producing a fin effect and fuel rod modeling in the code. The extent of these two factors cannot be quantitatively shown until the low flow, low void post-CHF convective heat transfer at these higher pressures is better defined. It can be concluded, however, that while the codes may currently calculate the quenches well, they do so for the wrong reasons.

## 6. REFERENCES

1. Grush, W. H.; Lin, J. C.; Linebarger, J. H.; and Nelson, R. A.; "Results and Predictions of Scaled, Nuclear Large Break Loss-of-Coolant Experiments," A paper submitted to the ASME 1980 Winter Annual Meeting, Chicago, Illinois.
2. "RELAP4/MOD6 A Computer Program for Transient Thermal-Hydraulic Analysis of Nuclear Reactors and Related Systems, User's Manual", CDAP-TR-003, May 1978<sup>a</sup>.

---

a. This EG&G Idaho, Inc. document is available from the NRC Public Document Room in Washington, D.C.

3. Nelson, R. A., "The Heat Transfer Surface Technique," presented at NRC sponsored LOCA Heat Transfer Workshop, Idaho Falls, Idaho, July 21-22, 1975.
4. Nelson, R. A. and Sullivan, L. H., "RELAP4/MOD6 Reflood Heat Transfer and Data Comparison," CSNI Specialists Meeting on Transient Two-Phase Flow, Paris, France, June 1978.
5. Nelson, R. A. and Sullivan, L. H., "Blowdown Heat Transfer Surface in RELAP4/MOD6 and Data Comparisons," ENS/ANS International Topical Meeting on Nuclear Power Reactor Safety, Vol. 2, Brussels, Belgium, October 1978, pp. 1719-1728.
6. Bjornard, T. A., "Blowdown Heat Transfer In A Pressurized Water Reactor," Ph.D. Thesis, M.I.T., August 1977.
7. Bjornard, T. A. and Griffith, P., "PWR Blowdown Heat Transfer," ASME Symposium on the Thermal and Hydraulic Aspects of Nuclear Safety, Vol. 1, November 27 - December 2, 1977, pp. 17-39.
8. Nukiyama, I., "Maximum and Minimum Values of Heat Transmitted from a Metal to Boiling Water Under Atmospheric Pressure," J. Soc. Mech. Eng. Japan, Vol. 37, 1934.
9. Bradfield, W. S., "Liquid-Solid Contact in Stable Film Boiling," I&EC Fundamentals, Vol. 5, May 1966, pp. 200-204.
10. Elias, E. and Yadigaroglu, G., "The Reflooding Phase of the LOCA in PWRs. Part II: Rewetting and Liquid Entrainment," Nuclear Safety, Vol. 19, No. 2, March-April 1978, pp. 160-175.
11. Elias, E.; Arrieta, L.; and Yadigaroglu, G.; "An Improved Model for the Rewetting of a Hot Fuel Rod," Trans. Am. Nucl. Soc., Vol. 24, 1976, pp. 299-300.

12. Kirchner, W. L., "Reflood Heat Transfer in a Light-Water Reactor," Ph.D. Thesis, M.I.T., January 1976; also NAC Report NUREG-0106, Vol. 1 and 2.
13. Iloeje, O. C.; Rohsenow, W. M.; and Griffith, P.; "Three-Step Model of Dispersed Flow Heat Transfer (Post CHF Vertical Flow)." ASME paper 75-WA/HT-1.
14. Dougall, R. S. and Rohsenow, W. M., "Film Boiling in the Inside of Vertical Tubes With Upward Flow of the Fluid At Low Qualities," M.I.T. Technical Report 9079-26.
15. Cheng, S. C.; Ny, W. W. L.; and Heng, K. T.; "Measurements of Boiling Curves of Subcooled Water Under Forced Convective Conditions," Int. J. Heat Mass Trans., Vol. 21, 1978, pp. 1385-1392.
16. Barnard, D. A.; Glastonbury, A. G.; and Ward, J. A.; "The Measurement of Post Dryout Heat Transfer at Low Pressure and Low Mass Quality Under Steady State Conditions," Paper at European Two-Phase Flow Group, Joint Research Center, ISPRA, June 1979.
17. Fung, K. K.; Gardiner, S. R. M.; and Groeneveld, D. C.; "Subcooled and Low Quality Flow Film Boiling of Water at Atmospheric Pressure," A paper accepted for publication in Nuclear Engineering and Design.
18. Rosal, E. R.; Hochreiter, L. E.; McGuire, M. F.; and Krepinevish M. C., "FLECHT Low Flooding Rate Cosine Test Series Data Report," Westinghouse Electric Corp. WCAP-8651, December 1975.
19. Comeau, J. G., "A Review of the Liedenfrost Phenomenon," Master of Mech. Eng. Report, Univ. of Ottawa, 1979.
20. Fung, K. K., "Post-CHF Heat Transfer During Steady-State and Transient Conditions," ANL-78-55, June 1978; also NUREG/CR-0195.



21. Gunnerson, F. S. and Cronenburg, A. W., "On the Thermodynamic Superheat Limit for Liquid Metals and Its Relation to the Liedenfrost Temperature," J. Heat Transfer, Vol. 100, November 1978, pp. 734-737.
22. Yao, S. C. and Henry, R. E., "An Investigation of the Minimum Film Boiling Temperature on Horizontal Surfaces," J. Heat Transfer, Vol. 100, May 1978, pp. 260-267.
23. Carslaw, H. and Jaeger, J., Conduction of Heat In Solids, 2nd Edition, Clarendon Press, Oxford, 1959.
24. Biasi, L., et al., "Studies on Burnout - Part 3," Energia Nuclear, Vol. 14, 1967, pp. 530-536.
25. Lin, J. C., "Posttest Analysis of LOFT Loss-of-Coolant Experiment L2-3," EG&G Idaho, Report No. EGG-LOFT-5075, March 1980<sup>a</sup>.
26. L. J. Siefken, FRAPT-T5 - A Computer Code for the Transient Analysis of Oxide Fuel Rods, NUREG/CR-0840, TREE-1281, June 1979.

---

a. This EG&G Idaho, Inc. document is available from the NRC Public Document Room in Washington, D.C.

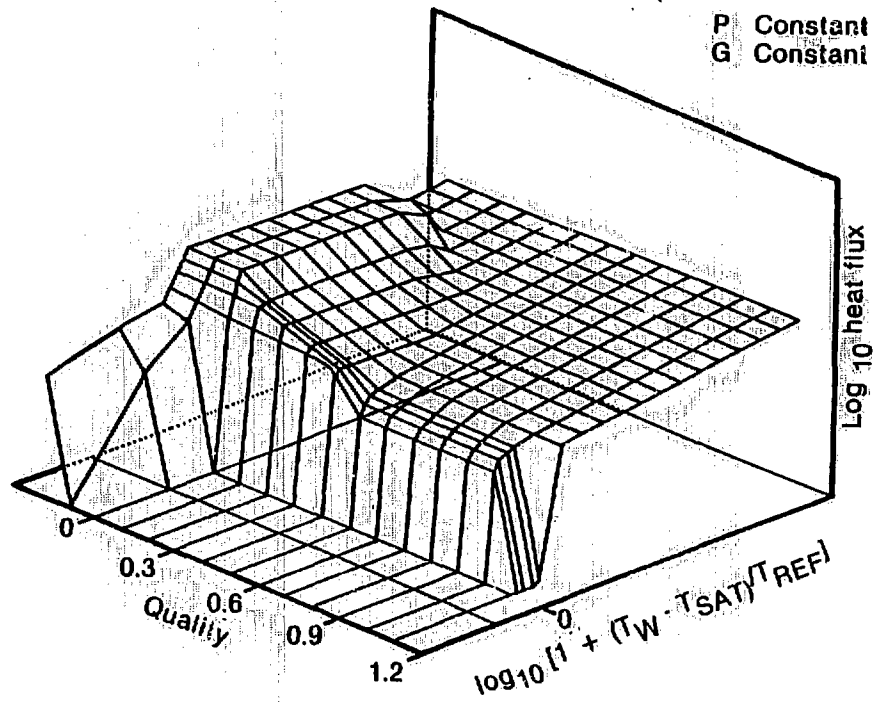
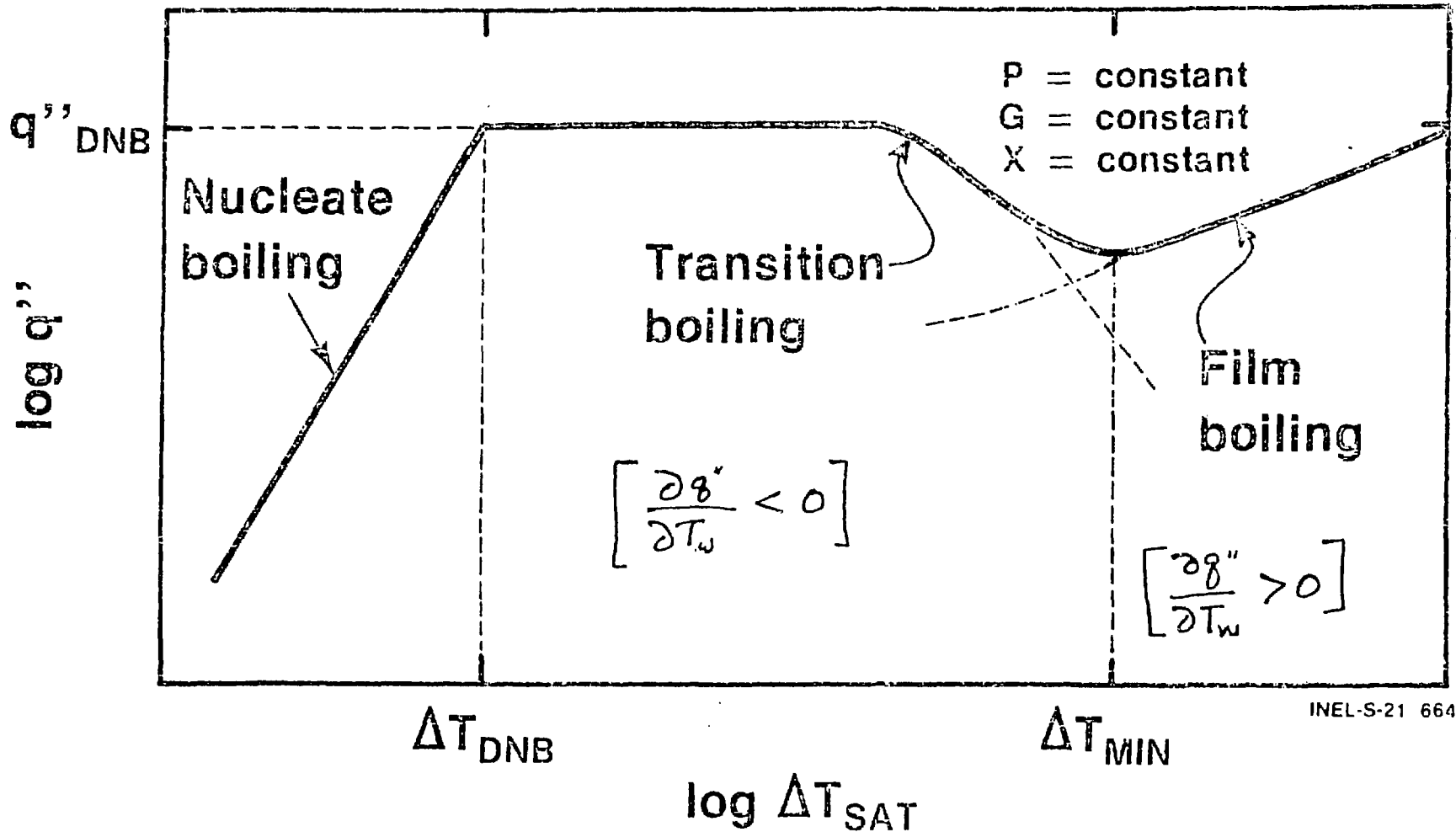


Figure 1. RELAP4/MOD6 blowdown heat transfer surface.



INEL-S-21 664

Figure 2. RELAP4/MOD6 Boiling Curve

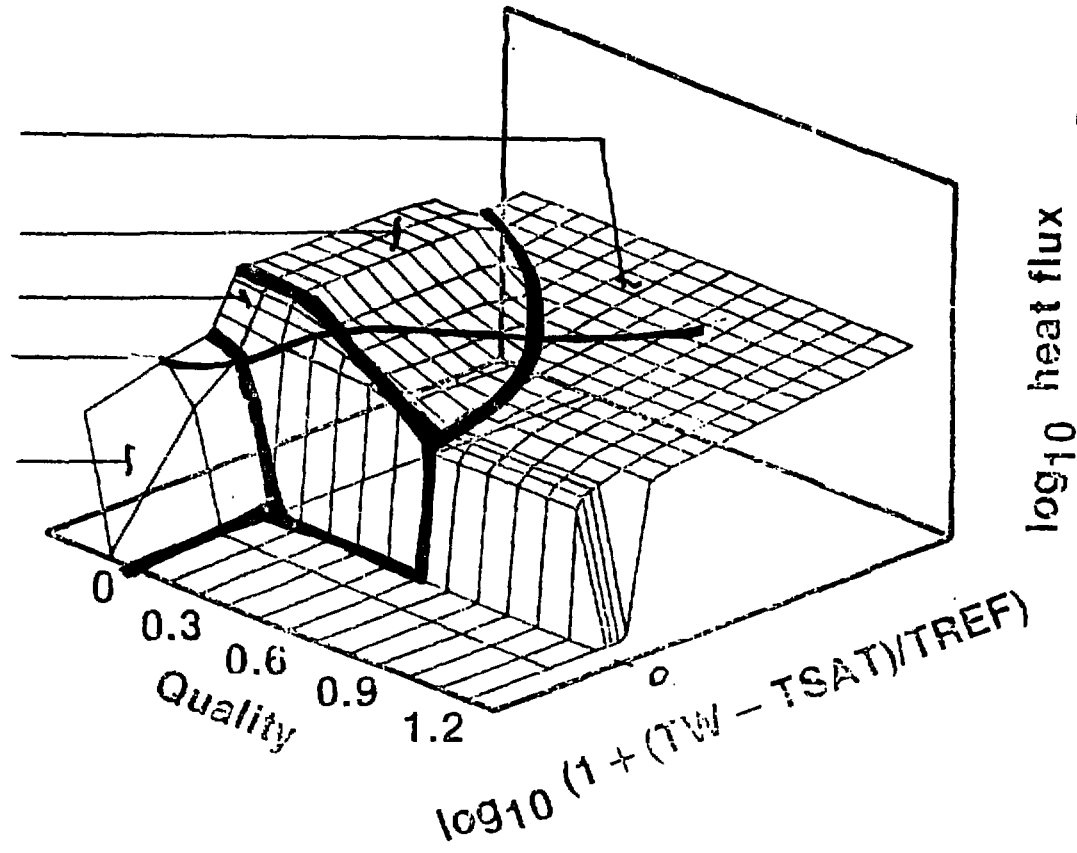
Film Boiling & Single  
Phase Vapor

Transition Boiling

Nucleate Boiling

Classical Pool Boiling  
Curve

Single Phase Liquid



P = constant  
G = constant

Figure 3. RELAP4/MOD6 Heat Transfer Regimes

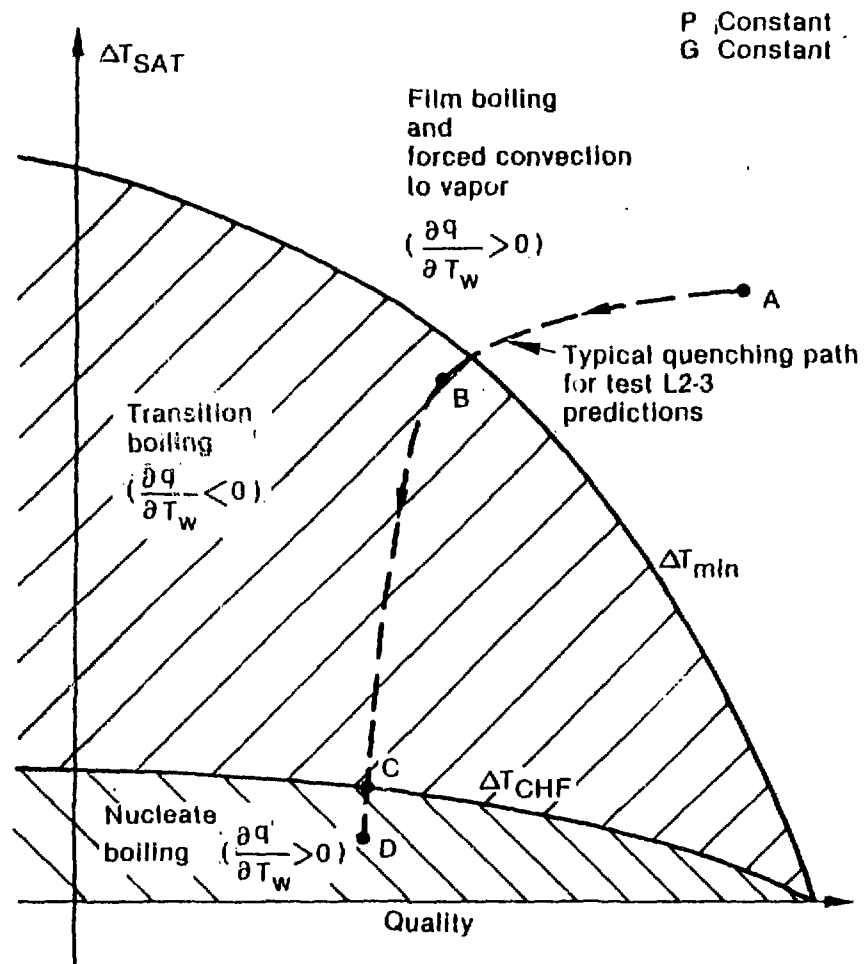


Figure 4. Loci of current maxima and minima of heat flux with respect to quality and subcooled.

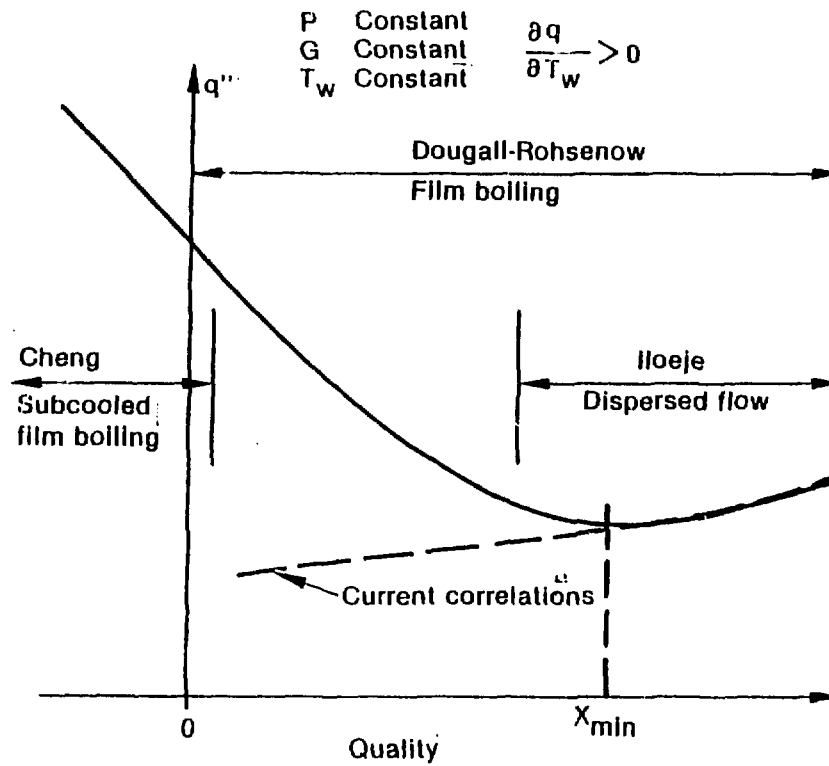


Figure 5. Synthesized Low Quality Affect on Film Boiling

<sup>6</sup> Figure 13 from Reference 16  
 Post dryout data,  $\dot{m}_a$ : Mass velocity =  $240 \text{ kg/m}^2\text{s}$   
 Upward flow: Wall temperature =  $500^\circ\text{C}$

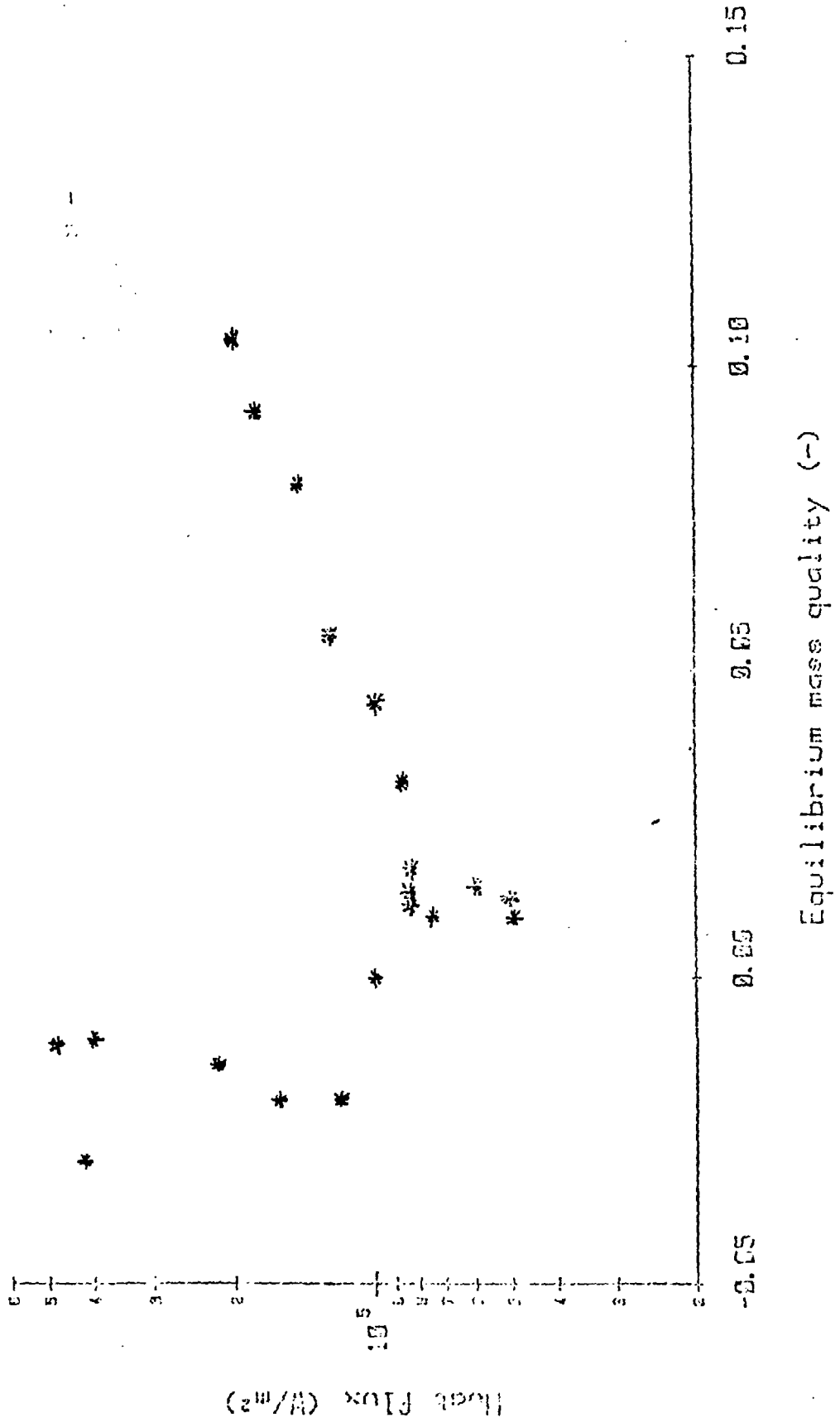
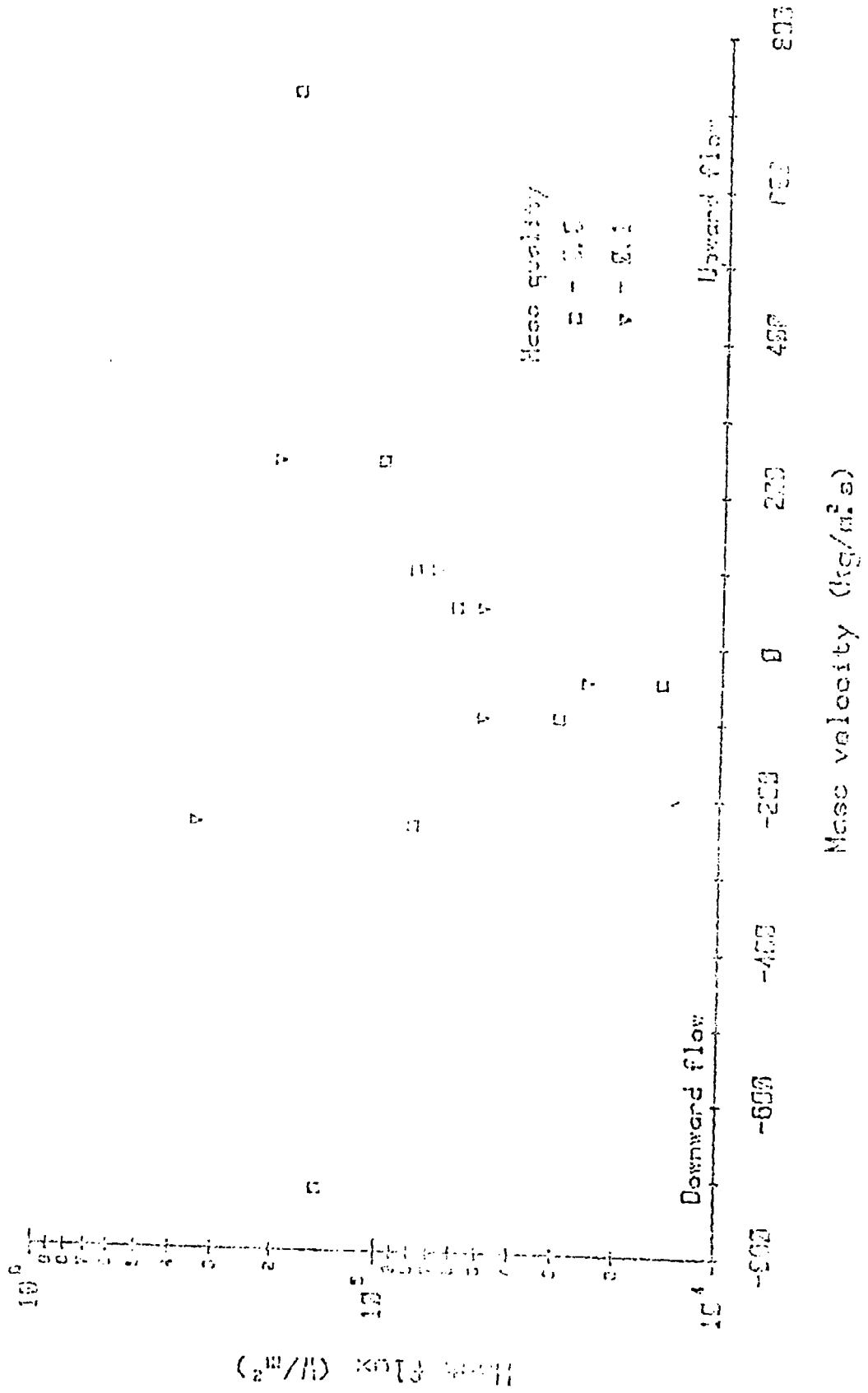


Figure 7

Effect of mass velocity and flow direction

Wall temperature = 500°C





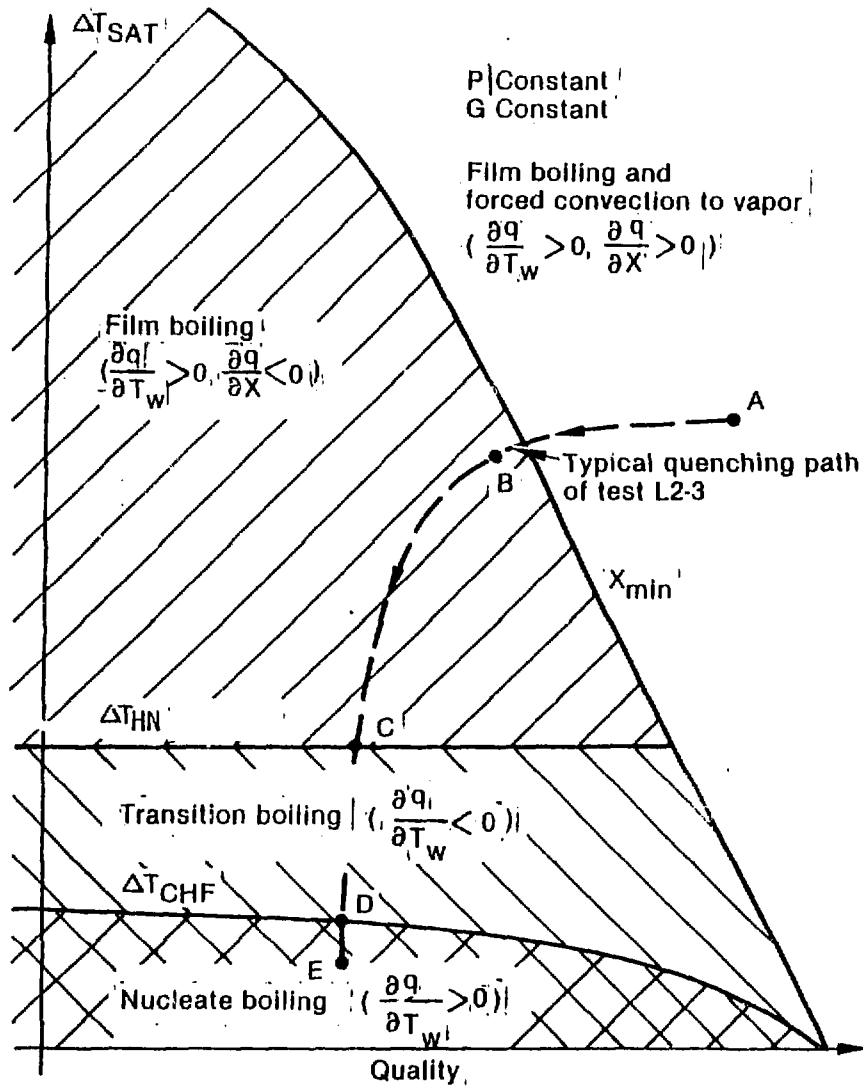


Figure 8. Loci of maxima and minima of heat flux with respect to quality and wall superheat showing effect of new mechanisms.

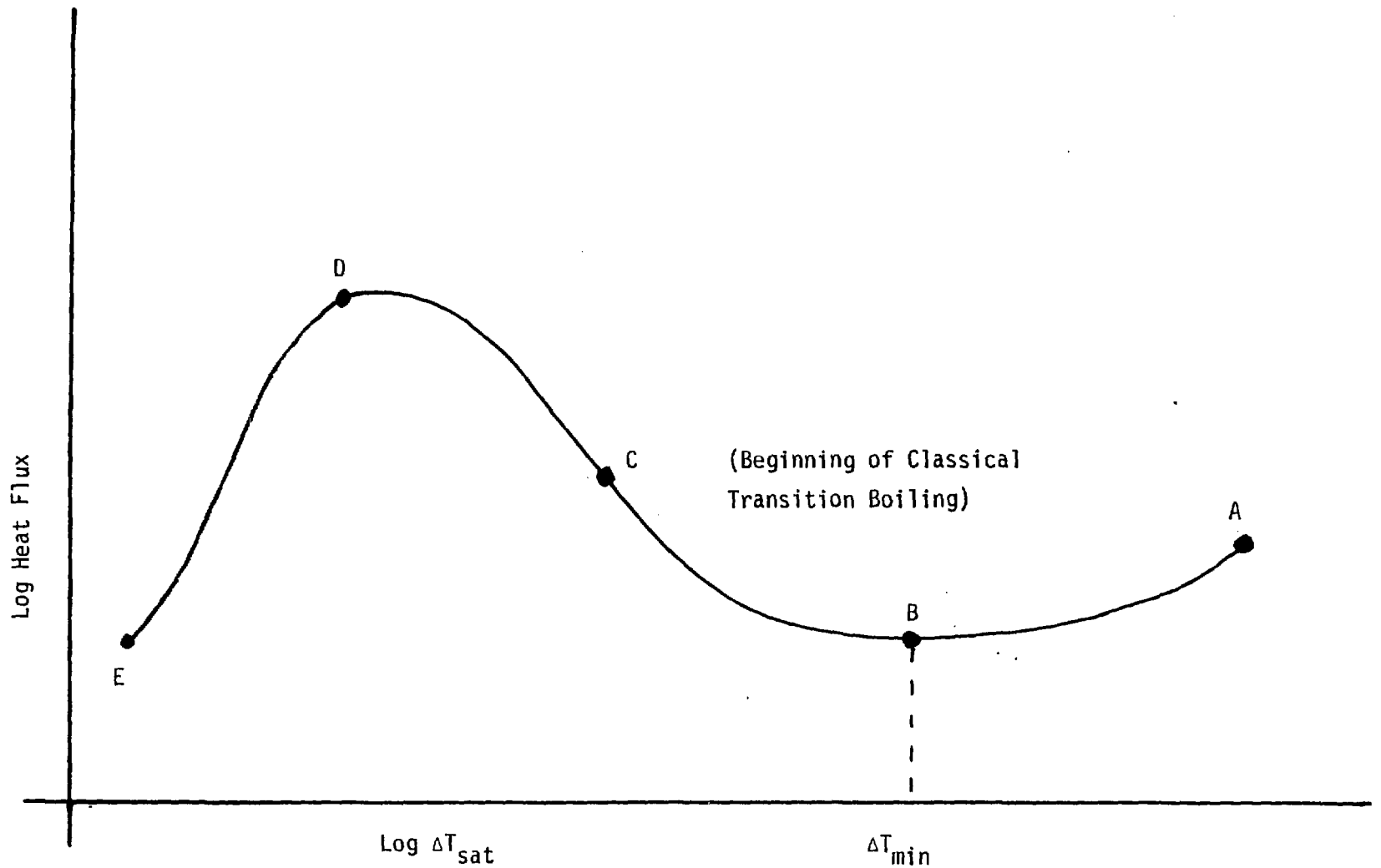


Figure 9. Plotting Classical Boiling Curve of Quench Neglecting Quality Variation

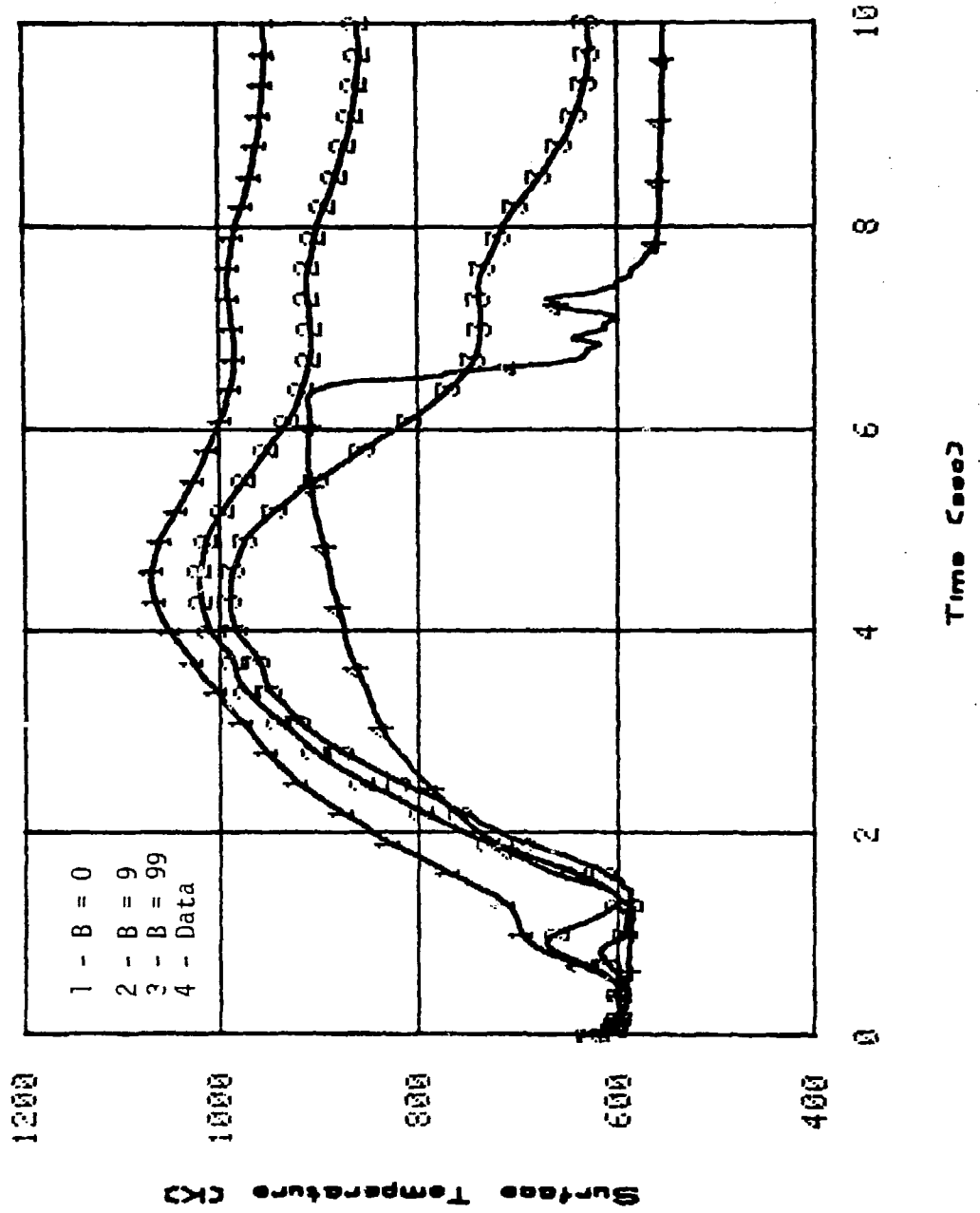


Figure 10. Results of Parametric Study on Hot Spot Temperature of Hot Pin for LOFT LB-1000